—Research Paper—

ZGLP1 Inhibits Proliferation and Migration of Smooth Muscle Cells and Promotes Apoptosis and Autophagy by Inhibiting Transforming Growth Factor Beta Receptor 1

ZHAOBIN ZENG, H. WANG, SHUTING WEN[1], RENHUI YI, J. CHEN[2], BANGMING GUO, Z. HU AND JIANYUN LOU*

Department of Neurosurgery, [1]Outpatient Department, [2]Department of Neurosurgery, First Affiliated Hospital of Gannan Medical University, Ganzhou, Jiangxi Province 341000, China

Zengzhao *et al*.: To Explore the Important Regulatory Role of ZGLP1

Intracranial aneurysm is a cerebrovascular-related disease with nearly half the mortality rate and is extremely destructive. It was suggesting that human aortic smooth muscle cells play important role in intracranial aneurysm. However, the regulation of human aortic smooth muscle cells is still unclear. To explore the important regulatory role of ZGLP1 in the development and progression of human aortic smooth muscle cells, cell counting kit-8 assay and cell cloning assays were used to detect cell proliferative capacity, and flow cytometry and Transwell assays were used for apoptosis and cell migration ability, respectively. The expression of autophagy protein was examined by Western blot to explore the relationship between ZGLP1 and autophagy. In addition, the targeting relationship between ZGLP1 and transforming growth factor beta receptor 1 was verified by constructing a transforming growth factor beta receptor 1 dual luciferase recombinant plasmid. Ox-ZGLP1 and si-ZGLP1 were transfected into human aortic smooth muscle cells respectively. The Ox-ZGLP1 group had significantly lower cell clone number, proliferative capacity and migration ability than the control group. Compared with the control, ox-ZGLP1s group showed a significant increase in apoptosis rate, and the expression levels of autophagy proteins light chain 3I and light chain 3II increased by about two times. Moreover, the luciferase reporter gene activity assay confirmed the interaction of ZGLP1 on transforming growth factor beta receptor 1. After co-transfection of oe-transforming growth factor beta receptor 1 and ox-ZGLP1, the proliferation and migration ability of human aortic smooth muscle cells decreased, while apoptosis and autophagy were increased. ZGLP1 can effectively inhibit the proliferation and migration of human aortic smooth muscle cells and down-regulate the apoptosis and autophagy of human aortic smooth muscle cells by down-regulating transforming growth factor beta receptor 1 *in vitro*.

Key words: Intracranial aneurysm, cell counting kit-8, transforming growth factor beta, cerebral thrombosis

An Intracranial Aneurysm (IA), a cerebral aneurysm, is often caused by abnormal bulging on the wall of the intracranial artery[1]. It ranks 3rd among cerebrovascular related diseases worldwide, 2nd only to cerebral thrombosis and hypertensive cerebral hemorrhage. Statistics show that 5 out of every 100 adults have an IA, nearly half of the patients with Ruptured Intracranial Aneurysms (RIA) die, and 30 % of the remaining survivors suffer from permanent neurologic deficit[2]. The currently known risk factors affecting IA include congenital dysplasia, hypertension and other mental factors[3],

but as a disease with high mortality and devastating disease, the pathogenesis of IA is still unclear. It was suggesting that Human Aortic Smooth Muscle Cells (HASMC) play important role in IA. However, the regulation of HASMC growth is still incomplete.

Transforming Growth Factor Beta Receptor 1 (TGFBR1) plays a crucial role in regulating various cellular processes, including cell proliferation,

*Address for correspondence
E-mail: zengzhaobin@gmu.cn

apoptosis, differentiation, migration and extracellular matrix production in HASMC. Specifically, TGFBR1 activates the TGF-beta signaling pathway, leading to downstream gene expression changes that play a role in arterial remodeling and cardiovascular disease. The signal transmitted by TGFBR1 triggers various processes of the cell, including cell growth, division, differentiation, and cell movement and apoptosis[4-7]. TGFBR1 is also involved in the process of tumor progression. MicroRNA (miR)-22 inhibits proliferation and differentiation of C2C12 myoblasts by targeting TGFBR1[8]. miR-3607-3p inhibits proliferation, migration and invasion of Non-Small Cell Lung Cancer (NSCLC) cells by targeting TGFBR1 and CCNE2[8]. TGFBR1 has been shown to promote migration and invasion of Michigan Cancer Foundation-7 (MCF-7) breast cancer cells, hepatocellular carcinoma and rectal cancer cells[9-11]. Studies have found that TGFBR1 signaling plays a critical role in the formation and progression of IA[12]. Specifically, mutations in TGFBR1 have been linked to the development of familial IA[12]. Additionally, TGFBR1 signaling has been found to contribute to the weakening of the arterial wall, which can lead to the formation of IA. Further research is needed to fully understand the role of TGFBR1 in IA.

From co-expression database, it was suggesting that ZGLP1 was negatively correlated with TGFBR1[13]. ZGLP1 encodes protein belonging to a transcriptional regulator family with GATA-like domain. So far, the role of ZGLP1 is still unclear. It was proved that ZGLP1 play vital role in the orogenic fate[14]. The GATA zinc finger transcription factors are a group of proteins that control gene expression in various developmental processes[15,16]. They play a particularly important role in regulating the development and differentiation of blood cells, as well as in the development of the heart, lungs and nervous system[17,18]. GATA factors are also involved in several pathological conditions like cancer and cardiovascular diseases[19]. Recent studies have provided the evidence that a zinc finger transcription factor, GATA-6 regulates the differentiation of vascular smooth muscle cells[20].

The aim of this study was to investigate the function of ZGLP1 in the HASMC and to explore the interaction between ZGLP1 and TGFBR1. Our results indicate that ZGLP1 affects the biological function of HASMC by down-regulating TGFBR1.

MATERIALS AND METHODS

Detection of transfection efficiency by quantitative Polymerase Chain Reaction (qPCR):

NucleoZol was added to the cell pellet for Ribonucleic Acid (RNA) extraction to detect RNA concentration, and the remaining samples were used for complimentary Deoxyribonucleic Acid (cDNA) synthesis. Real-time PCR amplification reactions were performed using SYBR Green Real-time PCR master mix. Relative quantitative analysis of the data according to the $2^{-\Delta\Delta Ct}$ method is performed as follows (x represents any sample):

$$\Delta\Delta Ct=(Ct.target–Ct.U6)x–(Ct.target–Ct.U6) control$$

Cell Counting Kit-8 (CCK-8) assay for cell proliferation:

After transfection of each group of cells, the cells were harvested for 24 h, and seeded in 96-well plates. 100 µl of 10 % CCK-8 solution was added to each well at five time points of 0, 24, 48, 72 and 96 h. Culture for 1 h~2h. The absorbance of each well was measured at Optical Density (OD) 450 nm by an enzyme-linked immunosorbent assay, and the inhibition rate of the cells was calculated.

Cell colony formation assay:

The cells in each experimental group in the logarithmic growth phase were trypsinized, and the whole medium was suspended to prepare a cell suspension, which was counted. The cells were seeded in a 6-well plate culture plate, and each experimental group was inoculated with 800 cells/well, and each experimental group was set with 3 replicate wells, and the medium was a complete medium containing 10 % Fetal Bovine Serum (FBS). Shake the inoculated cells and place them in an incubator to continue the culture. Change the cells every 3 d and observe the cell state. The clone size was observed under a microscope. When the number of cells in most of the individual clones in the well was greater than 50, the supernatant was discarded, and the cells were washed once with Phosphate Buffer Solution (PBS). 1 ml of 4 % paraformaldehyde was added to each well, and the cells were fixed in a 4° refrigerator for 60 min, and the cells were washed once with PBS. Add 1 ml of clean, impurity-free 0.1% crystal

violet dye solution to each well and stain the cells for 2 min. The cells were washed several times with double distilled Water (ddH$_2$O), dried, photographed by a digital camera, and cloned.

Flow cytometry:

The cells were washed twice with PBS pre-cooled at 4°, and the cells were resuspended in 250 µl of binding buffer to adjust the concentration to 1×106/ml. Take 100 µl of the cell suspension in a 5 ml flow tube and add 5 µl of Annexin V/Alexa Fluor 647 and 10 µl of 20 µg/ml propidium iodide solution. After mixing, incubate at room temperature for 15 min in the dark, add 400 µl of PBS to the reaction tube, and analyze by flow cytometry (Fluorescence-Activated Cell Sorting (FACS)).

Transwell assay:

After the cells were digested, they were resuspended in serum-free medium. Count and adjust the number of cells in each group to 1×105 cells/ml. 100 µl of the cell suspension was added to the upper surface of the Transwell chamber, 600 µl of medium containing 20 % FBS was added to the lower chamber and cultured in a 37° incubator. After 24 h, the upper chamber cells were wiped off with a cotton swab. In staining; remove the liquid from the upper and lower chambers, add 600 µl of 4 % paraformaldehyde to the lower chamber for 30 min, remove paraformaldehyde, wipe the cells that have not passed through the membrane with a cotton swab, and add 600 µl 0.1 % to the lower chamber. The crystal violet was stained for 15 min, and the chamber was washed twice with PBS. Each group was randomly selected under a microscope to take a picture, and the cells were observed and counted.

Western blot:

The collected cells were added to the Phenylmethylsulfonyl Fluoride (PMSF) containing protein lysate, allowed to stand on ice for 20 min, centrifuged at 12 000 rpm for 20 min at 4°, and the supernatant protein solution was taken 400 µl in the Eppendorf (EP) tube. The total protein concentration of the sample was measured by the Bicinchoninic Acid (BCA) protein assay. The protein molecular weight is differently configured with different concentrations of separation gel, and the concentrator is 4 %. After the Sodium Dodecyl Sulphate (SDS)-page gel is completely solidified, the comb is removed, placed in an electrophoresis tank, and the electrophoresis solution is filled. After the sample is applied, the voltage is stabilized at 90 V for 40 min, and the protein

marker is dispersed to adjust the voltage to 120 V. After the electrophoresis is completed, the target band is cut. An 8.5×6.5 cm nitrocellulose membrane (BioTrace, Pall, United States of America (USA)) was prepared for protein transfer. The transferred NC membrane protein was placed face up in 5 % Bovine Serum Albumin (BSA), shaken at 40 rpm, and blocked at room temperature for 2 h. After blocking, the NC membrane was placed in an antibody hybridization cassette containing primary antibody (β-actin, TGFBR1) and incubated overnight at 4° on a shaker. After the 2nd d of washing with Tris-Buffered Saline with 0.1 % Tween® 20 Detergent (TBST), the NC membrane was placed in a 1:5000 diluted rat secondary antibody hybridization cassette and incubated on a horizontal shaker for 2 h at room temperature. The NC membrane was placed flat on a transparent membrane, and the liquid A and the liquid B of the thermo Enhanced Chemiluminescence (ECL) kit were mixed in an equal volume and applied to the surface of the membrane, and left to stand in the dark for 3 min, and then the luminescent liquid on the membrane was removed and placed on the transparent membrane. Strip images were collected using a gel imaging system Versa Doc™ imaging system.

Construction of TGFBR1 dual luciferase recombinant plasmid:

According to the sequence of the 3' Untranslated Regions (3' UTRs) of the target gene found in GenBank, the primer was designed to be recombined into the psiCHECK™-2 dual luciferase reporter vector to construct a wild-type dual luciferase recombinant plasmid (TGFBR1-wide type). The specific binding sequence of the miRNA in the 3' UTRs of the target gene is the mutant double luciferase recombinant plasmid (TGFBR1-mutant type). The reporter gene in the psiCHECK™-2 dual luciferase reporter vector is the *Renilla* luciferase gene, and the control gene is the firefly luciferase gene.

Luciferase reporter gene activity assay:

Discard the old cell culture medium and add 100 µl of reporter cell lysate per well to fully lyse the cells. After the cells were lysed, each well was transferred to an EP tube and mixed by centrifugation. Slowly melt the firefly luciferase assay reagent and *Renilla* luciferase assay buffer to room temperature. The *Renilla* luciferase assay substrate (100×) was placed in an ice bath for later use. The *Renilla* luciferase assay substrate (100×) was added to the *Renilla* luciferase assay buffer at a ratio of 1:100 to prepare a *Renilla* luciferase assay working solution. Turn on the GLO-MAX 20/20 fluorescence

detector. When detecting firefly luciferase activity value F (firely Lueiferase), add 100 μl of firefly luciferase detection reagent to each cell sample, mix and place the EP tube immediately into the GLO-MAX 20/20 fluorescence detector to calculate the F value. Add 100 μl of *Renilla* luciferase assay solution, mix it and place it on the GLO-MAX 20/20 fluorescence detector to calculate *Renilla* luciferase activity value R (*Renilla* luciferase). After all sample measurements have been completed, the GLO-MAX 20/20 fluorescence detector calculates the relative luciferase activity F/R based on the previously detected F and R values.

Statistical methods:

GraphPad Prism® (GraphPad Sofware Inc) was used for statistical analysis, and each set of data was expressed as mean±standard deviation. To analyze differences between groups, independent sample t-test or one-way Analysis of Variance (ANOVA) were performed with statistical significance as follows, *$p<0.05$, ** $p<0.01$ and ***$p<0.001$.

RESULTS AND DISCUSSION

From co-expression database, it was suggesting that ZGLP1 was negatively correlated with TGFBR1 (fig. S1). The expression of ZGLP1 in the transfected cell line was detected by RT-PCR. To observe the effect of ZGLP1 on cell proliferation, cell cloning experiments and CCK-8 assay were performed. The results showed that the number of cell clones in the ox-ZGLP1 group was significantly lower than that in the mimic NC group ($p<0.01$). The number of cell clones in the si-ZGLP1 group was significantly increased ($p<0.001$). In addition, the ox-ZGLP1s group was compared with the control, and the proliferation ability of the cells decreased after 24, 48, 72 and 96 h of culture. Compared with the control, the si-ZGLP1 group increased the proliferation of cells after 24, 48, 72 and 96 h of culture.

The effect of ZGLP1 on HASMC cell migration was examined by transwell assay. The results showed that the migration ability of HASMC cells was significantly lower in the ox-ZGLP1s group compared with the control ($p<0.05$); si-ZGLP1 group compared with the control, the migration ability of the cells was significantly increased ($p<0.01$).

To test the effect of ZGLP1 on apoptosis, we used flow cytometry to detect apoptosis. The results showed that the apoptotic rate of the ox-ZGLP1s group was significantly higher than that of the control, which was about three times higher ($p<0.001$), while the si-ZGLP1 group was significantly lower than the control ($p<0.001$).

At the same time, the protein expression levels of autophagy-related proteins LC3I and LC3II were monitored by Western blot. The results showed that the expression levels of autophagy proteins LC3I and LC3II increased by about two-fold in the ox-ZGLP1s group compared with the control, with a significant increase ($p<0.01$). Compared with the control, the expression level of autophagy protein LC3I was significantly decreased by 3 fold ($p<0.001$), and the expression of LC3II was decreased by about 2 times ($p<0.01$).

After transfection of ox-ZGLP1, inhibitor NC and si-ZGLP1 in HASMC cells, the expression levels of TGFBR1 mRNA and protein were detected. The results showed that mRNA and protein levels of TGFBR1 were significantly decreased after transfection of ox-ZGLP1 ($p<0.01$). The realtime-PCR results showed that the expression level of TGFBR1 in the si-ZGLP1 group was significantly up-regulated by 3 fold ($p<0.01$), and the Western blot showed that the protein level was significantly increased by a factor of two ($p<0.01$).

AH-NC, oe-TGFBR1, mimic NC, ox-ZGLP1, oe-TGFBR1+ox-ZGLP1 and oe-TGFBR1+mimic NC were transfected into HASMC, respectively, and TGFBR1 expression levels were detected by qPCR and Western blot, respectively. The results showed that there was a significant increase in TGFBR1 mRNA expression and protein levels in the transfected oe-TGFBR1 group compared with the oe-NC group. Compared with the transfected oe-TGFBR1 group, the mRNA expression level of TGFBR1 was significantly decreased ($p<0.001$) after treatment with oe-TGFBR1 and ox-ZGLP1, which was reduced by half. Western blot analysis of TGFBR1 protein levels had the same results ($p<0.05$).

We further used the clone formation assay and CCK-8 assay to detect the effect of co-transfection of ox-ZGLP1 and TGFBR1 on the proliferation of HAMSC cells. The results showed that there was a significant increase in cell proliferation ability in the transfected oe-TGFBR1 group compared with the control group ($p<0.001$). The cell proliferation ability of co-transfected ox-ZGLP1 and TGFBR1 was reduced to the original level ($p<0.001$). The results of the CCK-8 method further indicated that the cells were treated with oe-TGFBR1 and ox-ZGLP1, and the cell

proliferation ability was significantly lower than that of the control group (p<0.05). On the other hand, the transwell assay detects changes in cell migration ability. The experimental results showed that the HASMC cell migration ability was significantly increased after transfection of oe-TGFBR1. After a total of oe-TGFBR1 and ox-ZGLP1, the cell migration ability was significantly reduced by more than one-fold (p<0.001).

To monitor the effect of co-transfection of oe-TGFBR1 and ox-ZGLP1 on the level of apoptosis, flow cytometry was performed to detect the level of apoptosis in HASMC cells. The results showed that the apoptosis rate of the oe-TGFBR1 group was significantly decreased (p<0.001). Compared with the control group, ox-ZGLP1 treatment showed a significant increase in apoptosis rate (p<0.001) and up-regulation by about four-fold. After treatment of HASMC cells with oe-TGFBR1 and ox-ZGLP1, the level of apoptosis was significantly increased (p<0.001).

In addition, Western blot was used to monitor the changes in protein expression levels of autophagy-associated proteins LC3I and LC3II after co-transfection of oe-TGFBR1 and ox-ZGLP1. Compared with the control group, the expression levels of the autophagy proteins LC3I and LC3II in the oe-TGFBR1 treated group were significantly decreased (p<0.001). The expression levels of autophagy proteins LC3I and LC3II in the ox-ZGLP1 treatment group increased (p<0.01). Co-transfection of oe-TGFBR1 and ox-ZGLP1 restored the expression levels of the proteins LC3I and LC3II.

An intracranial aneurysm is a disease with high mortality and devastating disease, and its pathogenesis is complex and unclear. It has been reported that HASMC play an important role in tumor development and migration. In this study, HASMC were used as experimental subjects to investigate the role of ZGLP, and to explore its underlying pathogenesis.

Studies have shown that TGF-beta receptors promote the formation of aneurysms[21-23]. At present, TGF-β signal transduction disorder is a common molecular marker related to the development of aortic aneurysm, which plays an important role in regulating blood vessel morphology[24,25]. Using the database to predict the negative regulatory genes of TGFBR1, we found that ZGLP1 was negatively co-expressed with TGFBR1. We hypothesized that ZGLP1 in HASMC may down regulate the transcription factor TGFBR1. Next, we investigated the effect of ox-ZGLP1 and TGFBR1 co-transformed with HASMC on the mRNA and protein levels of TGFBR1. As a result, the conclusion that the target gene of ZGLP1 is TGFBR1 is more reliable.

In this study, we first successfully constructed ox-ZGLP1 and ZGLP1 inhibitor transfected human aortic smooth muscle cell lines. To observe the effect of ZGLP1 on the biological function of HASMC, we used cell clone formation assay and CCK-8 assay to detect cell proliferation, and flow cytometry to detect apoptosis (fig. 1), cell migration ability was measured by transwell assay (fig. 2A and fig. 2B). The results indicate that ZGLP1 inhibits proliferation and migration of HASMC and promotes apoptosis of HASMC. It is well known that cancer is associated with an imbalance in autophagy. miRNAs are thought to be one of the potential regulatory elements that mediate autophagy pathways in cancer, and several studies have shown that miRNAs control autophagy of cancer cells through various biological pathways[26,27]. Therefore, it is necessary to explore the effect of ZGLP1 on the autophagy ability of cells. Western blotting was used to examine the effect of ZGLP1 on the expression levels of autophagy-related proteins LC3I and LC3II (fig. 2C-fig. 2E). The results confirmed that ZGLP1 promoted autophagy in HASMC (fig. 3).

To further validate the above hypothesis, this study explored the effects of ox-ZGLP1 and TGFBR1 co-transformed HASMC on cell biological function, and monitored the proliferation and migration of HASMC (fig. 4). The results indicate that ZGLP1 inhibits proliferation and migration of HASMC by inhibiting TGFBR1. What's more, flow cytometry was used to detect apoptosis after co-transfection, and western blot was used to detect changes in the expression levels of autophagy proteins LC3I and LC3II. The results showed that Ox-ZGLP1 promotes apoptosis and autophagy of HASMC by inhibiting TGFBR1 (fig. 5).

In conclusion, our results indicate that ZGLP1 effectively inhibits the proliferation and migration of HASMC *in vitro* and promotes apoptosis and autophagy in HASMC. Moreover, these effects are at least partially mediated by down-regulation of TGFBR1.
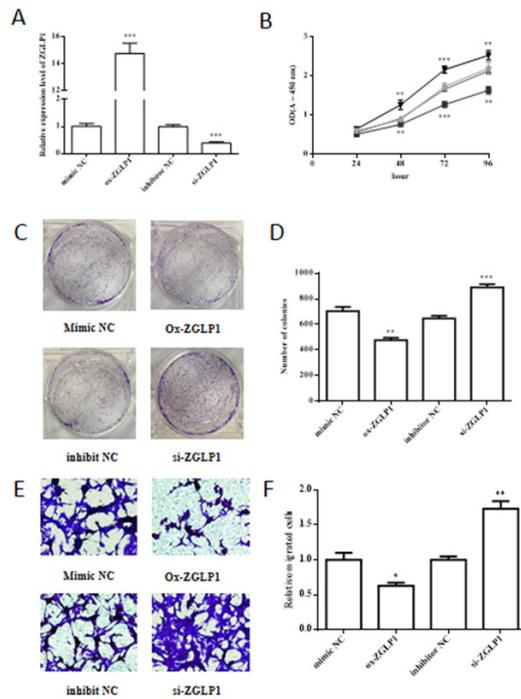
Fig. 1: ZGLP1 down-regulates the proliferation and migration of HASMC, (A): Ox-ZGLP1s and Si-ZGLP1 transfected cell lines were constructed in HASMC, and the expression of ZGLP1 was detected by qPCR; (B): CCK-8 method to detect the cell proliferation ability of each transfected cell line; (C and D): Cell cloning experiments were used to test cell proliferation ability and (E and F): Transwell assays were used to detect HASMC cell migration ability

Note: *p<0.05, **p<0.01 and ***p<0.001, ( ): mimic NC; ( ): Ox-ZGLP1; ( ): Inhibitor NC and ( ): si- ZGLP1
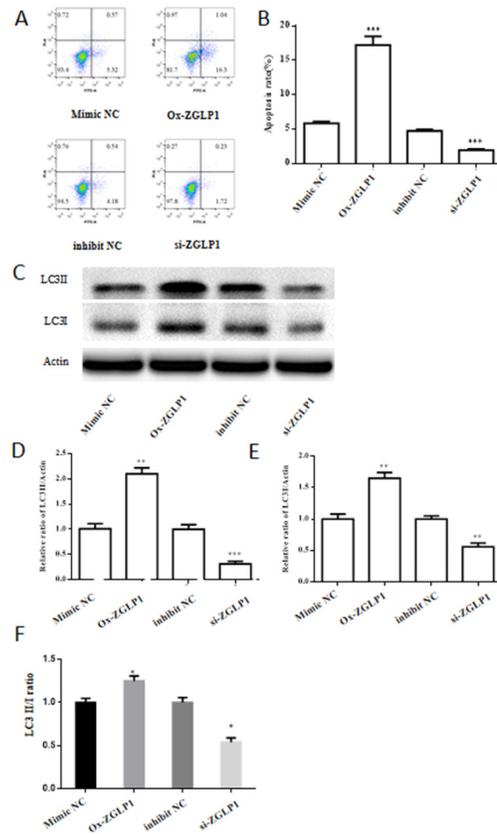
Fig. 2: ZGLP1 up-regulates the apoptotic level and autophagy of HASMC
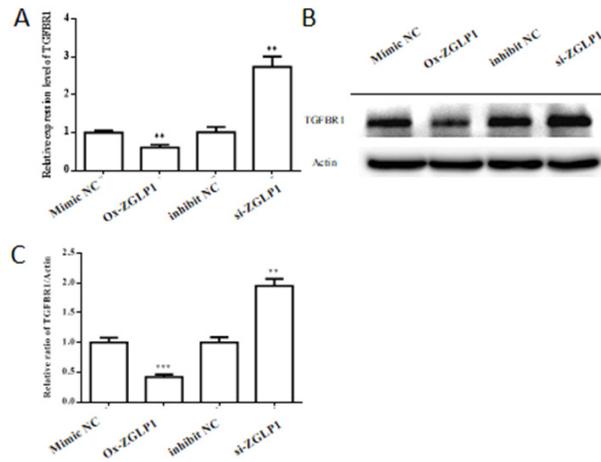
Fig. 3: ZGLP1 has a targeting relationship with TGFBR1. (A-C): After transfection of ox-ZGLP1, inhibitor NC and si-ZGLP1 in HASMC cells, the expression of TGFBR1 mRNA and protein were detected by qPCR and western blot, respectively and (D): Construction of the TGFBR1 dual luciferase recombinant plasmid to detect luciferase reporter gene activity
Note: **p<0.01 and ***p<0.001
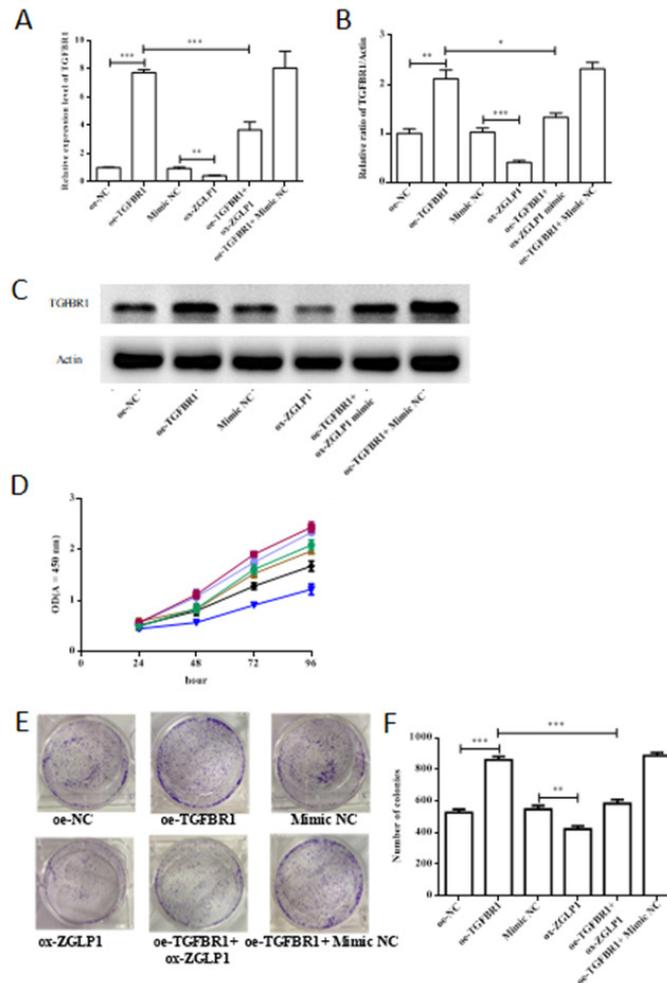
Fig. 4: Ox-ZGLP1 down-regulates the proliferation and migration of HASMC by inhibiting TGFBR1. (A-C): After co-transfection of oe-TGFBR1 and ZGLP1 mimic in HASMC, qPCR and Western blot were used to detect TGFBR1 mRNA and protein expression levels, respectively; (D): CCK-8 assay for cell proliferation and(E and F): Cloning formation experiments were used to detect cell proliferation
Note: *p<0.05, **p<0.01 and ***p<0.001, (●—): oe-NC; (■—): oe-TGFBR1; (▲—): mimic NC; (▼—): Ox-ZGLP1; (●—): oe-TGF-BR1+ox-ZGLP1 and (●—): oe-TGFBR1+mimic NC
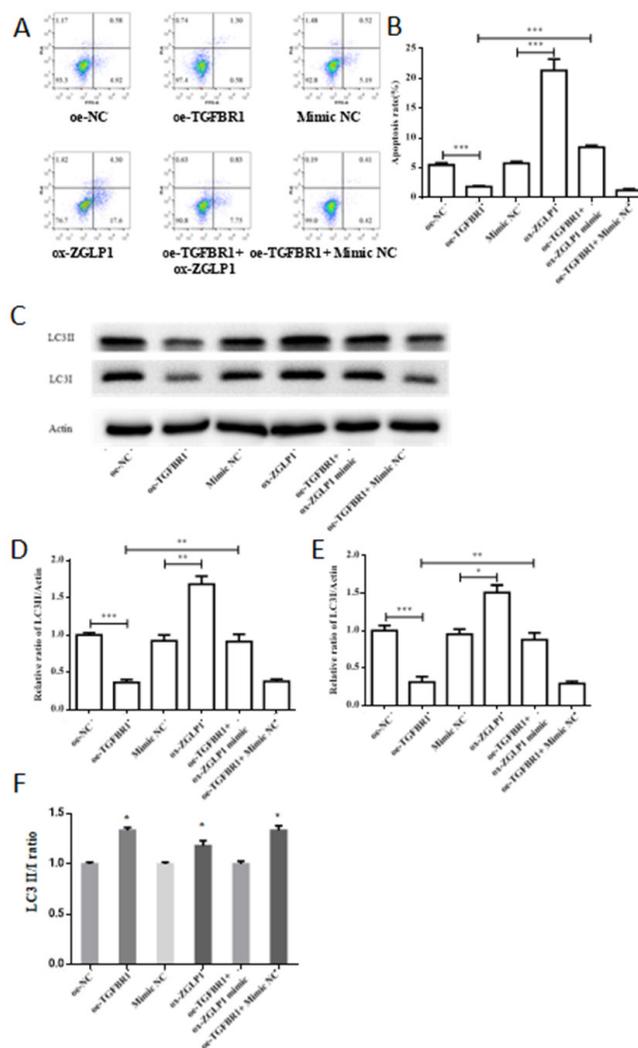
Fig. 5: Ox-ZGLP1 upregulates TGFBR1 upregulation of apoptotic levels and autophagy in HASMC. (A and B): After co-transfection of oe-TGFBR1 and Ox-ZGLP1, flow cytometry was performed to monitor the level of apoptosis in HASMC and (C-E): Western blot was used to detect changes in protein expression levels of autophagy-associated proteins LC3I and LC3II
Note: *p<0.05, **p<0.01 and ***p<0.001

Conflict of interests:

The authors declared no conflict of interests.

REFERENCES

1. Chalouhi N, Hoh BL, Hasan D. Review of cerebral aneurysm formation, growth, and rupture. Stroke 2013;44(12):3613-22.

2. Brisman JL, Song JK, Newell DW. Cerebral aneurysms. N Engl J Med 2006;355(9):928-39.

3. Francis SE, Tu J, Qian Y, Avolio AP. A combination of genetic, molecular and haemodynamic risk factors contributes to the formation, enlargement and rupture of brain aneurysms. J Clin Neurosci 2013 Jul 1;20(7):912-8.

4. Pasche B, Pennison MJ, Jimenez H, Wang M. TGFBR1 and cancer susceptibility. Transact Am Clin Climatol Assoc 2014;125:300-12.

5. Wang H, Zhang Q, Wang B, Wu W, Wei J, Li P, Huang R. miR-22 regulates C2C12 myoblast proliferation and differentiation by targeting TGFBR1. Eur J Cell Biol 2018;97(4):257-68.

6. Yu F, Chen B, Fan X, Li G, Dong P, Zheng J. Epigenetically-regulated microRNA-9-5p suppresses the activation of hepatic stellate cells via TGFBR1 and TGFBR2. Cell Physiol Biochem 2017;43(6):2242-52.

7. Cheng R, Dang R, Zhou Y, Ding M, Hua H. MicroRNA-98 inhibits TGF-β1-induced differentiation and collagen production of cardiac fibroblasts by targeting TGFBR1. Human Cell 2017;30:192-200.

8. Gao P, Wang H, Yu J, Zhang J, Yang Z, Liu M, et al. miR-3607-3p suppresses Non-Small Cell Lung Cancer (NSCLC) by targeting TGFBR1 and CCNE2. PLoS Genet 2018;14(12):e1007790.

9. Rosman DS, Phukan S, Huang CC, Pasche B. TGFBR1* 6A enhances the migration and invasion of MCF-7 breast cancer cells through RhoA activation. Cancer Res 2008;68(5):1319-28.

10. Li YU, Liu G, Li X, Dong H, Xiao W, Lu S. Long non-coding RNA SBF2-AS1 promotes hepatocellular carcinoma progression through regulation of miR-140-5p-TGFBR1 pathway. Biochem Biophys Res Commun 2018;503(4):2826-32.

11. Mody HR, Hung SW, Pathak RK, Griffin J, Cruz-Monserrate

Z, Govindarajan R. miR-202 diminishes TGFβ receptors and attenuates TGFβ1-induced EMT in pancreatic cancer. Mol Cancer Res 2017;15(8):1029-39.

12. Ruigrok YM, Baas AF, Medic J, Wijmenga C, Rinkel GJ. The transforming growth factor-β receptor genes and the risk of intracranial aneurysms. Int J Stroke 2012;7(8):645-8.

13. Zhu Q, Wong AK, Krishnan A, Aure MR, Tadych A, Zhang R, et al. Targeted exploration and analysis of large cross-platform human transcriptomic compendia. Nat Methods 2015;12(3):211-4.

14. Nagaoka SI, Nakaki F, Miyauchi H, Nosaka Y, Ohta H, Yabuta Y, et al. ZGLP1 is a determinant for the organic fate in mice. Science 2020;367(6482):eaaw4115.

15. Simon MC. Transcription factor GATA-1 and erythroid development. Proc Soci Exp Biol Med 1993;202(2):115-21.

16. Muntean AG, Ge Y, Taub JW, Crispino JD. Transcription factor GATA-1 and Down syndrome leukemogenesis. Leuk Lymphoma 2006;47(6):986-97.

17. Cantor AB, Orkin SH. Coregulation of GATA factors by the Friend of GATA (FOG) family of multitype zinc finger proteins. Semin Cell Dev Biol 2005;16(1):117-28.

18. Pikkarainen S, Tokola H, Kerkelä R, Ruskoaho H. GATA transcription factors in the developing and adult heart. Cardiovasc Res 2004;63(2):196-207.

19. Fujiwara T. GATA transcription factors: Basic principles and related human disorders. Tohoku J Exp Med 2017;242(2):83-91.

20. Wada H, Hasegawa K, Morimoto T, Kakita T, Yanazume T, Sasayama S. A p300 protein as a coactivator of GATA-6 in the transcription of the smooth muscle-myosin heavy chain gene. J Biol Chem 2000;275(33):25330-5.

21. Yang P, Schmit BM, Fu C, DeSart K, Oh SP, Berceli SA, et al. Smooth muscle cell-specific Tgfbr1 deficiency promotes aortic aneurysm formation by stimulating multiple signaling events. Sci Rep 2016;6(1):35444.

22. Lucarini L, Sticchi E, Sofi F, Pratesi G, Pratesi C, Pulli R, et al. ACE and TGFBR1 genes interact in influencing the susceptibility to abdominal aortic aneurysm. Atherosclerosis 2009;202(1):205-10.

23. Baas AF, Medic J, Van't Slot R, De Kovel CG, Zhernakova A, Geelkerken RH, et al. Association of the TGF-β receptor genes with abdominal aortic aneurysm. Eur J Hum Gene 2010;18(2):240-4.

24. Jaffe M, Sesti C, Washington IM, Du L, Dronadula N, Chin MT, et al. Transforming growth factor-β signaling in myogenic cells regulates vascular morphogenesis, differentiation, and matrix synthesis. Arterioscl Thromb Vasc Biol 2012;32(1):e1-1.

25. Choudhary B, Ito Y, Makita T, Sasaki T, Chai Y, Sucov HM. Cardiovascular malformations with normal smooth muscle differentiation in neural crest-specific type II TGFβ receptor (Tgfbr2) mutant mice. Dev Biol 2006;289(2):420-9.

26. Ren Y, Chen Y, Liang X, Lu Y, Pan W, Yang M. MiRNA-638 promotes autophagy and malignant phenotypes of cancer cells via directly suppressing DACT3. Cancer Lett 2017;390:126-36.

27. Baur K, Wolf P, Riener R, Duarte JE. Making neurorehabilitation fun: Multiplayer training via damping forces balancing differences in skill levels. In2017 Inte Conf Rehabil Robot 2017;2017:876-81.